analytical chemistry

Letter

Cite This: Anal. Chem. XXXX, XXX, XXX-XXX

pubs.acs.org/ac

Antibody-Templated Assembly of an RNA Mimic of Green Fluorescent Protein

Alessandro Bertucci, Alessandro Porchetta, and Francesco Ricci*

Department of Chemical Sciences and Technologies, University of Rome Tor Vergata, Via della Ricerca Scientifica 1, 00133, Rome, Italy

Supporting Information

ABSTRACT: One of the most intriguing ways through which nature achieves regulation of biological pathways encompasses the coordination of noncovalent interactions that bring biomolecules to be colocalized in a designated restricted space. Inspired by this mechanism, we have explored the possibility of using antibodies as bivalent biomolecular substrates for the templated assembly of a functional RNA structure. We have developed a biosupramolecular complementation assay by assembling a fluorescent Spinach aptamer, which is a synthetic RNA mimic of the Green Fluorescent Protein, from its split segments. We have employed two antigen-tagged RNA strands that, upon binding to the target antibody, are colocalized in a confined space and can reassemble into the native Spinach conformation, yielding a measurable fluorescence emission as a function of the templating antibody concentration. We have demonstrated the generality of our approach using two different antigen/antibody systems and found that both platforms show high binding affinity, specificity for the target antibody, and enough selectivity to work in crude cellular extracts. This study highlights the potential of biosupramolecular RNA engineering for the development of innovative biomimetic tools for nanobiotechnology and bioanalytical assays.

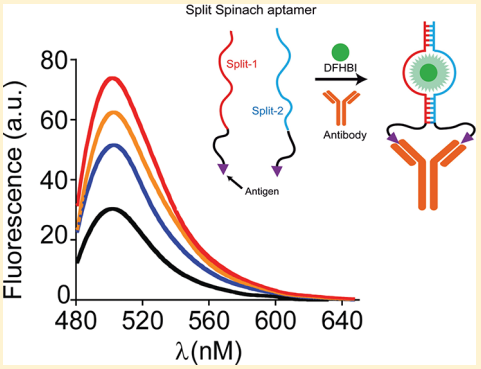

In living systems information is stored, transferred, and processed through a complex network of reactions that involve thousands of different species. In order to preserve the functionality of cells, this sophisticated system has to be controlled and regulated in a highly specific and precise way. To do this, nature has developed refined strategies based on noncovalent interactions that allow biomolecules to be colocalized in an extremely confined volume, which results in an increase of their effective local concentrations.[1,2] Such local concentration enhancement triggers reactions and promotes interactions that would otherwise be negligible at the low concentration levels found in cells.[2−4] Inspired by this mechanism, spatial colocalization of interacting species has been artificially recreated to generate hierarchical architectures and to seize control of synthetic reactions.[5−7] This proximity-based strategy has been successfully employed for biosupramolecular assembly[8−10] and templated organic synthesis.[11,12] It also has seen growing application in bioanalytical chemistry and synthetic biology.[13−16] One of the best examples of colocalization-based assembly is the protein-fragment complementation assay. This method allows for monitoring biomolecular interactions through the use of a reporter protein initially split into two halves, each one tethered to a specific recognition element. The interaction between the two recognition elements, or with a third interactive species, induces the colocalization-based assembly of the protein halves into the active protein conformation, which can then report on the interaction event (Figure S1).[17,18] On the basis of this mechanism, the bioassisted assembly of a Split Green Fluorescent Protein (split GFP) has been proposed as a protein reporter system for the analysis of protein−protein interactions,[19] the intracellular detection of target nucleic acids,[20] and the creation of semisynthetic assembling proteins.[21] However, split GFP-based techniques do not come without limitations. The conjugation of the GFP fragments to the desired recognition element may prove challenging.[22] Moreover, GFP fragments may be susceptible to self-aggregation, which lowers the amount of competent split GFP fragments and then the probability of interaction-dependent reassembly.[19,23] Recently, a synthetic RNA structure has been proposed as an alternative system to GFP. Such a GFP-mimic RNA aptamer, named Spinach, specifically binds to a synthetic copy (3,5-difluoro-4-hyroxybenzylidene imidazoline, DFHBI) of the natural GFP fluorophore, leading to the display of GFP-like fluorescence properties.[24] Spinach and related Spinach-like daughter structures have since then emerged as groundbreaking biochemical tools and been employed for real-time imaging of RNA transcription,[25] detection of cellular metabolites,[26] and monitoring of dynamic bioprocesses.[27] Inspired by the above colocalization mechanism, split Spinach complementation strategies have been proposed in which the

Received: June 2, 2017
Accepted: November 13, 2017

DOI: 10.1021/acs.analchem.7b02102
Anal. Chem. XXXX, XXX, XXX−XXX

assembly of the functional aptamer is controlled by nucleic acid strand displacement reactions[28,29] or guided by the hybridization with complementary mRNA strands.[30] However, there are no reports of split Spinach assembly strategies using proteins as biomolecular templates. Motivated by the above considerations, we demonstrate here a strategy for the antibody-templated assembly of a functional RNA structure mimicking the fluorescent properties of GFP. Because of their bivalent recognition-site structure, antibodies represent privileged substrates to assist colocalization-based assembly.[13] We thus propose the use of a split Spinach aptamer (GFP-like RNA mimic) as a flexible and dynamic tool to design a complementation assay that is responsive to target antibodies.

TEMPLATED ASSEMBLY OF A SPLIT SPINACH APTAMER USING AN ANTI-DIG ANTIBODY

Our strategy is based on the use of two RNA strands that, when joined together, constitute the active conformation of the Spinach aptamer. Each of the two Spinach fragments is conjugated at one end with a ligand (i.e., an antigen) that is recognized by a specific antibody. In the absence of the antibody, the two Spinach fragments display a very weak luminescent signal because of the poor binding affinity for DFHBI. The interaction between the target antibody and the RNA-conjugated antigens brings the two RNA strands in close proximity, which greatly increases their effective local concentration. This ultimately triggers the assembly of the functional Spinach structure and leads to efficient binding of DFHBI with consequent increase of the fluorescence signal (Figure 1 and Figures S1 and S2).

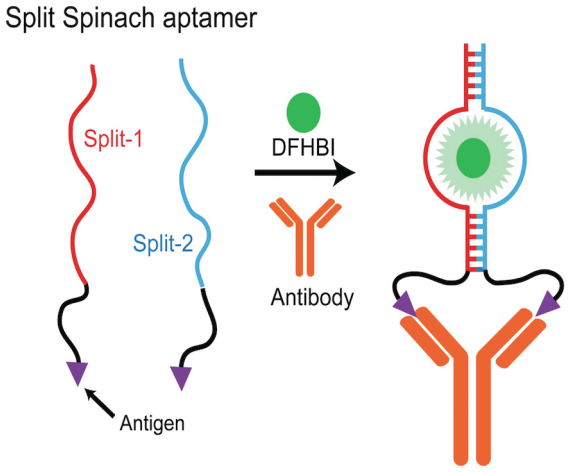

Figure 1. Antibody-templated assembly of the Spinach aptamer. In this strategy, Spinach is ideally cut into two segments (red and blue in the figure),[32] and each of the two fragments is conjugated with a recognition element (antigen) specific for a target antibody. Only in the presence of the antibody the two fragments are colocalized in a confined volume and can reassemble into the functional Spinach aptamer which, by binding to the fluorophore DFHBI, provides a GFP-like fluorescence signal.

As a test bed, we initially focused on digoxigenin (Dig) as the recognition element (antigen) and Anti-Dig antibody as the biomolecular target (Figure 2A). Given the proof-of-principle nature of this study, we used here the original minimized version of the Spinach aptamer,[31] which was recently employed for split Spinach assembly controlled by strand displacement reactions.[28] The actual crystal structure of this Spinach aptamer, which significantly differs from simplified *in silico* models, has been elucidated and reported by Ferré-D'Amaré and coworkers (see Figure S2).[32] We split up the original single strand RNA aptamer into two fragments (Split-1 and Split-2) by executing an ideal cut along the stem of the so-called P3 paired region.[32] This region of the Spinach structure is more prone to undergo sequence modification without significant loss of the DFHBI binding activity (i.e., activation of fluorescence emission), due to its sole structural role. In particular, the reported crystal structure has evidenced that a G-quadruplex folding, formed upon interactions of the bases in the other regions of the Spinach, is necessary for competent DFHBI binding, thus leaving the P3 region as the only suitable one for structural modifications.[28,31,32] Additional spacer tails composed of 10 uracil units were introduced at the 5′-terminus of Split-1 and at the 3′-terminus of Split-2 (i.e., in correspondence of the base of the main stem P1 of the Spinach aptamer), in order to endow the two RNA segments with enough flexibility once they are bound to the target antibody (Figure 1 and Figure S2 RNA sequences are reported in the Supporting Information). A Dig molecule is then conjugated to each of these spacer tails (Figure 2A). In the absence of the target antibody, an equimolar solution of Split-1 and Split-2 (20 nM) shows an affinity toward DFHBI (K_d = 17 ± 2 μM) that is 10-fold poorer than that of the original native aptamer (K_d = 1.6 ± 0.1 μM) (Figure 2B). This demonstrates that the split Spinach configuration shows only a poor DFHBI binding ability which, consequently, leads to very weak signaling for DFHBI concentrations as high as 10 μM (Figure 2B, black curve). However, in the presence of Anti-Dig antibody (20 nM), the affinity of the split Spinach for DFHBI is restored to a value (K_d = 3.3 ± 0.4 μM) approaching that of the original wild-type aptamer, thus providing evidence for the proposed mechanism. The small difference in DFHBI affinity between the antibody-templated Spinach and the original aptamer may be ascribed to a slight destabilization of the Spinach structure induced by the presence of the additional poly-U tails as well as to possible steric hindrance caused by the antibody structure. Further proof of the proposed antibody-templated assembly of the split Spinach is given by the result obtained using Anti-Dig Fab fragments, which feature only one binding site instead of the traditional two of the complete Anti-Dig IgG antibody. In this case, addition of the Fab fragments to the Anti-Dig-tagged RNA strands did not yield any measurable increase in the fluorescence output (Figure 2F). No improvement on DFHBI affinity could be achieved compared to the split Spinach configuration, even at saturating concentrations of the Anti-Dig Fab (100 nM) (Figure S3). In order to find the optimal experimental conditions for our antibody-templated assembly, we compared the signal gains % obtained in the presence of a fixed concentration of Anti-Dig antibody (20 nM), at different DFHBI concentrations. A concentration of 3 μM DFHBI yields the highest signal gain (175%), which is in accordance with the affinity curve for DFHBI (Figure 2B) and with the lower background signal due to split Spinach (see also Figures S5 and S6). However, we note that, because of the difference in affinity, a higher DFHBI concentration (10 μM) provides more intense, and thus more reliable, absolute fluorescence signals despite a slightly lower total signal gain (125%) (Figure 2C and Figure S7). The obtained fluorescence gains account for the fact that, statistically, only half of the total amount of Split-1 and Split-2 is thought to bind to the receptor

DOI: 10.1021/acs.analchem.7b02102
Anal. Chem. XXXX, XXX, XXX−XXX

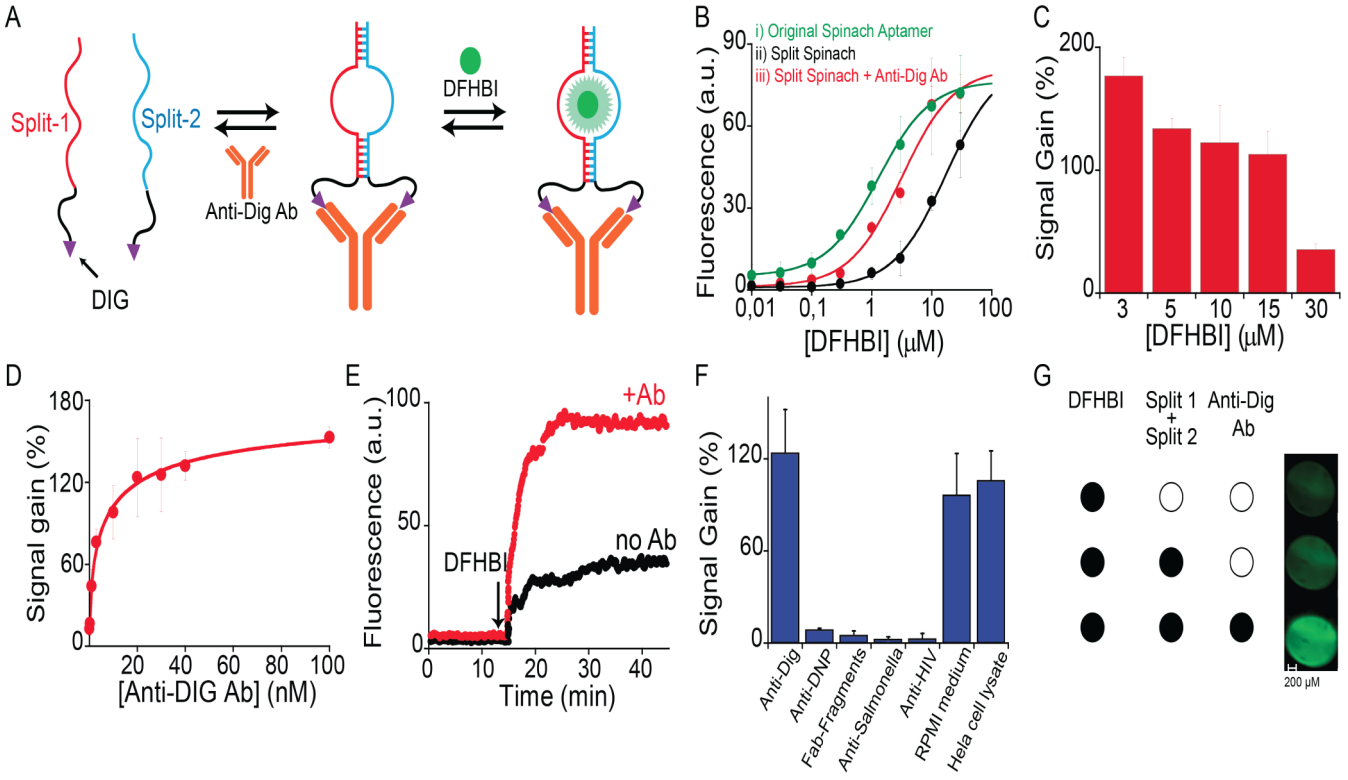

Figure 2. Antibody-templated assembly of the Spinach aptamer. (A) We first employed Digoxigenin (Dig) as the recognition tag and Anti-Dig antibody as the target antibody. (B) DFHBI binding curves of Split Spinach in absence (black) and presence of Anti-Dig antibody (20 nM) (red). As a comparison, the original wild-type Spinach aptamer (green) is also shown. (C) Fluorescence % signal gains in the presence of Anti-Dig antibody (20 nM) obtained at different DFHBI concentrations. (D) Binding curve at increasing Anti-Dig antibody concentrations. (E) Fluorescence kinetics profiles of the split spinach aptamer in absence (black line) and in the presence of Anti-Dig antibody 100 nM (red line). (F) Cross reactivity experiments using different antibodies demonstrate the high specificity of the system. Moreover, the system responds to the specific Anti-Dig antibody (20 nM) in RPMI cell culture medium or HeLa Cell whole lysate with similar performances compared to those observed in pure buffer solution. (G) Representative fluorescence microscopy micrographs of the progressive phases of the assembly process (1.5 μL droplets, exposure time 10 s). Scale bar is 200 μm. Signal gain is calculated as the fluorescence intensity enhancement upon addition of the Anti-Dig antibody, relative to the Split Spinach background fluorescence signal in the presence of DFHBI (10 μM). Unless otherwise noted the experiments are obtained in phosphate buffer saline PBS buffer, pH 7.4, T = 37 °C, using an equimolar concentration of the split strands ([split 1] = [split 2] = 20 nM) and a concentration of DFHBI of 10 μM. Results are reported as mean value of three independent measurements and the error bars reflect the standard deviations.

sites in a complementary fashion (thus assembling into Spinach), with the remaining part leading to homologous noninteracting Split-1/Split-1 or Split-2/Split-2 combinations. This is in accordance with a fluorescence turn-on ratio lower than that observed for split Spinach systems assembled on templating mRNA strands.[30] As we anticipated, at higher DFHBI concentrations (i.e., above 15 μM), the signal gain was largely suppressed due to the strong background fluorescence (Figure 2C). Additionally, we investigated the behavior of our system using different concentrations of split Spinach in the presence of either 3 μM or 10 μM DFHBI, and found that 20 nM RNA ensured the highest signal gain %, namely, the best signal-to-noise ratio (Figures S5 and S6). We observed a concentration-dependent increase of Spinach fluorescence emission at increasing concentrations of Anti-Dig antibody, showing nanomolar affinity ($K_{1/2}$ = 5 ± 1 nM,Figure 2D). Affinity binding curves showing the increase of fluorescence intensity as a function of antibody concentration are included in the Supporting Information (Figure S7). The above affinity binding value is in good accordance with the one reported in the literature obtained with different assays, such as ELISA.[33] Kinetic profiles showed that the Spinach assembly triggered by the presence of Anti-Dig antibody leads to rapid binding of DFHBI, yielding 90% of the final signal in less than 5 min (Figure 2E).

We then tested our system against nonspecific cross reactivity. Saturating concentrations (100 nM) of nonspecific antibodies induced no variation in terms of signal gain, demonstrating the high specificity of our approach (Figure 2F). In view of further biomedical applications, we also tested the performances of the assembly process both in RPMI cell culture medium and HeLa Cell whole lysate. Notably, the fluorescence signal gains obtained working in these complex biomatrixes were comparable with those registered in pure buffer solution (Figure 2F). Fluorescence microscopy analysis confirmed that bright green fluorescence emission is achieved only when in the presence of the specific target antibody, which suggests the potential use of this technology for bioimaging and bioanalytical purposes (Figure 2G).

ANTI-DNP-TEMPLATED SPLIT SPINACH ASSEMBLY

Motivated by the above results, we tested our technology using a second antigen−antibody couple, in order to demonstrate the general applicability of the proposed approach. We employed 2,4-dinitrophenol (DNP) tags that are recognized by the specific Anti-DNP antibody. DNP-modified Split Spinach

DOI: 10.1021/acs.analchem.7b02102
Anal. Chem. XXXX, XXX, XXX−XXX

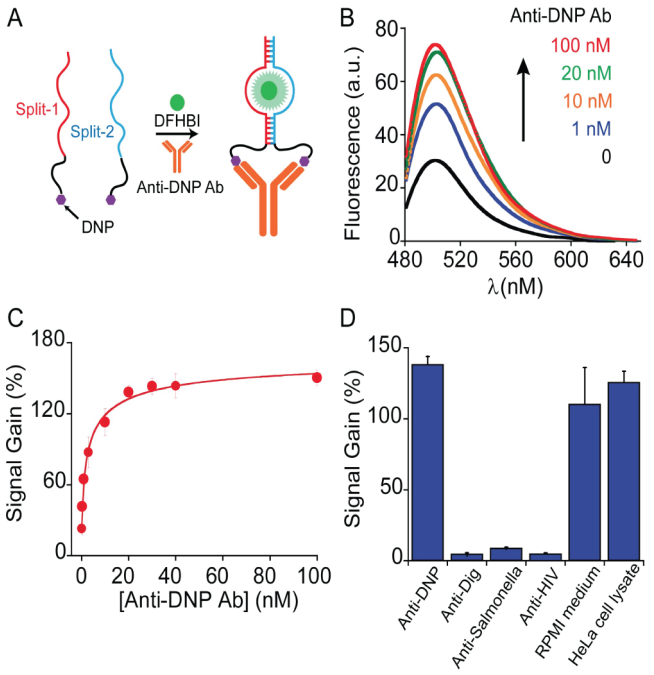

Figure 3. (A) Split-spinach assembly templated by an Anti-DNP antibody; (B) fluorescence emission spectra of the assembled Spinach-DFHBI complex as a function of the concentration of the Anti-DNP antibody, (C) binding curve at increasing Anti-DNP antibody concentrations, and (D) cross-reactivity experiments carried out with different nonspecific antibodies. The Anti-DNP-based assembly system also works in complex biomatrixes such as RPMI medium or HeLa Cell whole lysate. All reported fluorescence intensities are relative to background DFHBI signal considered as blank sample (10 μM). Unless otherwise noted the experiments are obtained in phosphate buffer saline PBS buffer, pH 7.4, T = 37 °C, using an equimolar concentration of the split strands ([split 1] = [split 2] = 20 nM) and a concentration of DFHBI of 10 μM. Results are reported as mean value of three independent measurements, and the error bars reflect the standard deviations.

segments were designed as for the above Dig-labeled RNA strands (Figure 3A). Following the same experimental protocol, we recorded fluorescence emission spectra that demonstrated that the same colocalization-based assembly of the split Spinach is achieved using Anti-DNP antibodies. Fluorescence emission (Figure 3B) and signal gains % comparable to those registered for Anti-Dig antibodies were obtained. Moreover, the binding curve obtained at increasing concentrations of Anti-DNP antibody also showed nanomolar affinity ($K_{1/2}$ = 2.1 ± 0.4 nM, Figure 3C and Figure S6), in accordance with the literature values.[34] We demonstrated again that the assembly of the Spinach structure is triggered only by the presence of the specific target antibody (here Anti-DNP antibody), as we observed no fluorescence enhancement at saturating concentrations of nonspecific antibodies (Figure 3D). The use of RPMI and HeLa Cell whole lysate as matrices did not affect the performance of the Anti-DNP-assisted assembly and we observed comparable signal gains to those obtained in pure buffer solution (Figure 3D).

CONCLUSIONS

We have presented a biosupramolecular mechanism in which a split Spinach is led to reassemble into the functional RNA GFP-mimic conformation as the effect of a guided spatial nanoconfinement. We demonstrated the applicability of this approach using antibodies as template biomolecules that induce colocalization of split Spinach halves, mediated by the binding of antigen tags conjugated to the ends of the RNA fragments. Looking forward, modification of the design may be explored to improve the fluorescence background of split Spinach, for instance through the introduction of different split points, variable length of the uracil tails, or different base pairing in the P3 region. We also believe the same mechanism might be translated to some of the available alternative formats of the Spinach aptamer.[32,35,36] More advanced designs may account for peptide/RNA chimeras to extend this strategy to a wider range of target antibodies, allowing for the development of even more robust tools for colocalization-based sensing. This would also allow orthogonal assembly of diversified RNA mimics of GFP activated by different antibodies.

Given the crucial role that nucleic acids and proteins play when employed together as building blocks for the semi-synthetic assembly of functional nanostructures,[37] we believe our strategy may find different possible applications. Our colocalization mechanism may be extended to other RNA aptamers and sequences, opening the way to the construction of programmable supramolecular RNA-based nanostructures with binding-responsive properties, which is of high relevance in the field of RNA nanotechnology. Looking forward, we believe that the presented Spinach complementation assay might find application as a means to perform in situ imaging of antibodies and other bivalent cellular receptors. Despite this work being a proof-of-principle study, we in fact envision that an analogous mechanism could be explored in the future to generate new sets of colocalization-based probes. This would allow, for instance, for imaging of B-cell receptors (BCRs) on the surface of B-cells, leading to their visualization *in situ* in real-time.[38] Likewise, imaging of other bivalent cellular receptors (e.g., tyrosine kinases) might be achieved by using properly designed ligand-tagged RNA strands.[39] Eventually, we believe our strategy may be valid for a large number of other substrates, namely, all those proteins that display bi- or multivalency and are then amenable to assist colocalization assembly. Given this, a split Spinach complementation assay may be developed for intracellular imaging of RNA- and aptamer-binding proteins, being then fully genetically encodable. This would allow this technology to be further implemented as an expressible signaling system.

ASSOCIATED CONTENT

Supporting Information

The Supporting Information is available free of charge on the ACS Publications website at DOI: 10.1021/acs.analchem.7b02102.

RNA sequences, materials and methods, data analysis, split Spinach aptamer assay scheme, illustration of the sequence of the split Spinach aptamer used, binding curve for DFHBI of the Split Spinach system, fluorescence emission spectra, signal gain % as function of concentration of split Spinach in presence of respective equimolar concentrations of Anti-Dig antibody, raw fluorescence intensity of split Spinach in the concentration range 10−30 nM, and binding curves for increasing antibody concentrations (PDF)

DOI: 10.1021/acs.analchem.7b02102
Anal. Chem. XXXX, XXX, XXX−XXX

AUTHOR INFORMATION

Corresponding Author

*E-mail: francesco.ricci@uniroma2.it.

ORCID

Francesco Ricci: 0000-0003-4941-8646

Author Contributions

A.B. and A.P. contributed equally. All authors have given approval to the final version of the manuscript.

Notes

The authors declare no competing financial interest.

ACKNOWLEDGMENTS

This work was supported by Associazione Italiana per la Ricerca sul Cancro, AIRC (Project No. 14420, F.R.) and by the European Research Council, ERC (Project No. 336493, F.R.). We thank Alessia Amodio for helpful support with fluorescence microscopy.

REFERENCES

(1) Mattia, E.; Otto, S. *Nat. Nanotechnol.* **2015**, *10*, 111−119.
(2) Kuriyan, J.; Eisenberg, D. *Nature* **2007**, *450*, 983−990.
(3) Pawson, T.; Scott, J. D. *Science* **1997**, *278*, 2075−2080.
(4) Bhattacharyya, R. P.; Reményi, A.; Yeh, B. J.; Lim, W. A. *Annu. Rev. Biochem.* **2006**, *75*, 655−680.
(5) Petkau-Milroy, K.; Brunsveld, L. *Org. Biomol. Chem.* **2013**, *11*, 219−232.
(6) Fu, J.; Liu, M.; Liu, Y.; Yan, H. *Acc. Chem. Res.* **2012**, *45*, 1215−1226.
(7) Bromley, E. H.; Channon, K.; Moutevelis, E.; Woolfson, D. N. *ACS Chem. Biol.* **2008**, *3*, 38−50.
(8) Bosmans, R. P.; Briels, J. M.; Milroy, L. G.; de Greef, T. F.; Merkx, M.; Brunsveld, L. *Angew. Chem.* **2016**, *128*, 9045−9049.
(9) Chidchob, P.; Edwardson, T. G.; Serpell, C. J.; Sleiman, H. F. *J. Am. Chem. Soc.* **2016**, *138*, 4416−4425.
(10) Kukolka, F.; Schoeps, O.; Woggon, U.; Niemeyer, C. M. *Bioconjugate Chem.* **2007**, *18*, 621−627.
(11) Barluenga, S.; Winssinger, N. *Acc. Chem. Res.* **2015**, *48*, 1319−1331.
(12) Li, X.; Liu, D. R. *Angew. Chem., Int. Ed.* **2004**, *43*, 4848−4870.
(13) Zhang, H.; Li, F.; Dever, B.; Wang, C.; Li, X. F.; Le, X. C. *Angew. Chem., Int. Ed.* **2013**, *52*, 10698−10705.
(14) Tsai, C. T.; Robinson, P. V.; Spencer, C. A.; Bertozzi, C. R. *ACS Cent. Sci.* **2016**, *2*, 139−147.
(15) Nagaraj, S.; Wong, S.; Truong, K. *ACS Synth. Biol.* **2012**, *1*, 111−117.
(16) Williams, B. A.; Diehnelt, C. W.; Belcher, P.; Greving, M.; Woodbury, N. W.; Johnston, S. A.; Chaput, J. C. *J. Am. Chem. Soc.* **2009**, *131*, 17233−17241.
(17) Paulmurugan, R.; Umezawa, Y.; Gambhir, S. S. *Proc. Natl. Acad. Sci. U. S. A.* **2002**, *99*, 15608−15613.
(18) Paulmurugan, R.; Gambhir, S. S. *Anal. Chem.* **2003**, *75*, 1584−1589.
(19) Magliery, T. J.; Wilson, C. G.; Pan, W.; Mishler, D.; Ghosh, I.; Hamilton, A. D.; Regan, L. *J. Am. Chem. Soc.* **2005**, *127*, 146−157.
(20) Tyagi, S. *Nat. Methods* **2007**, *4*, 391−392.
(21) Sakamoto, S.; Kudo, K. *J. Am. Chem. Soc.* **2008**, *130*, 9574−9582.
(22) Tyagi, S. *Nat. Methods* **2009**, *6*, 331−338.
(23) Blakeley, B. D.; Chapman, A. M.; McNaughton, B. R. *Mol. BioSyst.* **2012**, *8*, 2036−2040.
(24) Paige, J. S.; Wu, K. Y.; Jaffrey, S. R. *Science* **2011**, *333*, 642−646.
(25) Pothoulakis, G.; Ceroni, F.; Reeve, B.; Ellis, T. *ACS Synth. Biol.* **2014**, *3*, 182−187.
(26) Strack, R. L.; Song, W.; Jaffrey, S. R. *Nat. Protoc.* **2014**, *9*, 146−155.
(27) Höfer, K.; Langejürgen, L. V.; Jäschke, A. *J. Am. Chem. Soc.* **2013**, *135*, 13692−13694.
(28) Rogers, T. A.; Andrews, G. E.; Jaeger, L.; Grabow, W. W. *ACS Synth. Biol.* **2015**, *4*, 162−166.
(29) Bhadra, S.; Ellington, A. D. *RNA* **2014**, *20*, 1183−1194.
(30) Ong, W. Q.; Citron, Y. R.; Sekine, S.; Huang, B. *ACS Chem. Biol.* **2017**, *12*, 200−205.
(31) Paige, J. S.; Nguyen-Duc, T.; Song, W.; Jaffrey, S. R. *Science* **2012**, *335*, 1194−1194.
(32) Warner, K. D.; Chen, M. C.; Song, W.; Strack, R. L.; Thorn, A.; Jaffrey, S. R.; Ferré-D'Amaré, A. R. *Nat. Struct. Mol. Biol.* **2014**, *21*, 658−663.
(33) (a) Janissen, R.; Berghuis, B. A.; Dulin, D.; Wink, M.; van Laar, T.; Dekker, N. H. *Nucleic Acids Res.* **2014**, *42*, e137. (b) Derks, R. J. E.; Hogenboom, A. C.; Van Der Zwan, G.; Irth, H. In *Emerging Technologies in Protein and Genomic Material Analysis*; Marko-Varga, G., Oroszlan, P., Eds. Elsevier: Amsterdam, The Netherlands, 2003; p 90.
(34) (a) Jung, H.; Yang, T.; Lasagna, M. D.; Shi, J.; Reinhart, G. D.; Cremer, P. S. *Biophys. J.* **2008**, *94*, 3094−3103. (b) Bilgiçer, B.; Moustakas, D. T.; Whitesides, G. M. *J. Am. Chem. Soc.* **2007**, *129*, 3722−3728.
(35) Huang, H.; Suslov, N. B.; Li, N. S.; Shelke, S. A.; Evans, M. E.; Koldobskaya, Y.; Rice, P. A.; Piccirilli, J. A. *Nat. Chem. Biol.* **2014**, *10*, 686−691.
(36) Filonov, G. S.; Moon, J. D.; Svensen, N.; Jaffrey, S. R. *J. Am. Chem. Soc.* **2014**, *136*, 16299−16308.
(37) Niemeyer, C. M. *Angew. Chem., Int. Ed.* **2010**, *49*, 1200−1216.
(38) Mallikaratchy, P. R.; Ruggiero, A.; Gardner, J. A.; Kuryavyi, V.; Maguire, W. F.; Heaney, M. L.; McDevitt, M. R.; Patel, D. J.; Scheinberg, D. A. *Nucleic Acids Res.* **2011**, *39*, 2458−2469.
(39) (a) Yuzawa, S.; Opatowsky, Y.; Zhang, Z.; Mandiyan, V.; Lax, I.; Schlessinger, J. *Cell* **2007**, *130*, 323−334. (b) Lemmon, M. A.; Schlessinger, J. *Cell* **2010**, *141*, 1117−1134.

DOI: 10.1021/acs.analchem.7b02102
Anal. Chem. XXXX, XXX, XXX−XXX